Article

Coincubation as miR-loading strategy to improve the anti-tumor effect of stem cell-derived EVs

Alessia Brossa[1,2], Marta Tapparo[2], Valentina Fonsato[2,3], Elli Papadimitriou[1,2], Michela Delena[2], Giovanni Camussi[4], Benedetta Bussolati[1,2]

[1]Department of Molecular Biotechnology and Health Sciences, University of Torino, Torino, Italy
[2]Molecular Biotechnology Center, University of Torino, Torino, Italy
[3]2i3T, Società per la gestione dell'incubatore di imprese e per il trasferimento tecnologico, Torino, Italy
[4]Department of Medical Science; University of Torino, Torino, Italy.

* Correspondence: Tel. 011-6706453, e-mail: benedetta.bussolati@unito.it.

Abstract: Extracellular vesicles are considered a novel therapeutic tool, due to their ability to transfer their cargoes to target cells. Different strategies to directly load extracellular vesicles with RNA species have been proposed. Electroporation has been used for the loading of non-active vesicles, however the engineering of vesicles already carrying a therapeutically active cargo is still under investigation. We here set up a coincubation method to increase the anti-tumor effect of extracellular vesicles isolated from human liver stem cells (HLSC-EVs). Using the coincubation protocol, vesicles were loaded with the anti-tumor miRNA-145, and their effect was evaluated on renal cancer stem cell invasion. Loaded HLSC-EVs maintained their integrity and miR transfer ability, and miR-145 was protected by RNAse digestion possibly due to its binding to RNA-binding proteins on HLSC-EV surface, such as Annexin A2. Moreover, miR-145 coincubated HLSC-EVs were more effective in inhibiting the invasive properties of cancer stem cells, in comparison to naïve vesicles. The protocol reported here exploits a well described property of extracellular vesicles to bind nucleic acids on their surface and protect them from degradation, in order to obtain an effective miRNA loading that results in the increase of the effect of naïve active extracellular vesicles.

Keywords: extracellular vesicle engineering, microRNA, loading, anti-tumor, cancer stem cells, exosomes, coincubation

1. Introduction

Extracellular vesicles (EVs) are nanosized vesicles actively released by many, if not all, cells and identified in biological fluids [1]. EVs display the ability to deliver active cargo, including RNA species, to target cells thus reprogramming their gene expression profile [2]. Therefore, the interest for the exploitation of EVs as therapeutic tool is rapidly increasing. Indeed, EVs appear a highly efficient delivery system, as compared to delivery of naked molecules, as they protect the cargo from degradation by RNases and proteases [3, 4]. Moreover, in comparison to synthetic liposomes, EVs might display an increased efficacy since, being a natural cell derived product, they show reduced clearance by the macrophagic system, low immunogenicity and ability to deliver nucleic-acid-based therapeutics across biological barriers [5, 6].

A great effort has been therefore dedicated to the pharmacological exploitation of EVs as carriers of specific cargo of interest [7]. In particular, EV engineering with RNA species has been proposed for different therapeutic applications, ranging from anti-tumor strategies to vaccination [4, 8, 9]. Different technical approaches for EV loading include the option to modify the originating cell, typically by transfection, or to directly load isolated EVs using electroporation [4]. The approach of direct EV

loading might be of particular interest in those contexts where the delivery of the identified cargo represents the main mechanism of action of the therapeutic preparation. For instance, we recently set up a methodology for direct electroporation of EVs isolated from plasma for the loading of antitumor microRNAs without perturbation of their integrity and targeting properties [10]. In this context, the use of plasma derived EVs from an autologous source might appear of therapeutic relevance.

A different situation can be envisaged when EVs carrying *per se* a therapeutically active cargo are loaded with a desired molecule to increase their effect. We recently showed that EVs from human liver stem cells (HLSC) induced a potent anti-tumor effect *in vitro* and *in vivo* [11-14]. Specifically, HLSC-EVs inhibited the invasion of renal cancer stem cells (rCSCs) [14], and induced their apoptosis [12]. Preliminary experiments attempting to load HLSC-EVs with an additional miR cargo trough electroporation not only failed to increase their therapeutic effect, but rather reduced it, suggesting the loss of their endogenous activity.

The aim of the present paper was therefore to identify a strategy to potentiate the endogenous anti-tumor activity of stem-cell derived EVs avoiding the loss of their endogenous effect. For this purpose, exploiting the EV ability to bind, protect and transport active RNA species on their surface, we set up a co-incubation protocol able to load microRNAs on HLSC-EVs and to increase their anti-tumor effects.

2. Materials and Methods

2.1 Renal Cancer Stem Cells isolation and culture.

Renal cancer stem cells (rCSCs) were isolated and characterized as previously described [12, 14, 15]. Cells were obtained from specimens of renal cell carcinomas from patients undergoing nephrectomy, according to the Ethics Committee of the S. Giovanni Battista Hospital of Torino, Italy (168/2014). CD105 positive rCSCs were isolated by magnetic cell sorting from the total tumor cell population, using the magnetic-activated cell sorting (MACS) system (Miltenyi Biotec, Auburn, CA, USA). Single CD105 positive cells were seeded in 96-well plates in presence of the expansion medium, consisting of DMEM LG (Invitrogen, Carlsbad, CA, USA), supplemented with 2 nM L-glutamine (Lonza, Basel, Switzerland), insulin-transferrin-selenium, 10-9 M dexamethasone, 100 U penicillin, 1000 U streptomycin, 10 ng/ml epidermal growth factor (EGF) (all from Sigma-Aldrich, St.Louis, MO, USA) and 5% fetal calf serum (FCS) (Euroclone, MI, Italy). A CD105 positive clonal rCSC line was selected and used for all the experiments, as previously described [12, 14]. Mycoplasma absence was routinely tested using RT-PCR.

2.2 Human Liver Stem Cells isolation and culture

Human Liver Stem Cells (HLSCs) were generated by Anemocyte International (Gerenzano, Italy) from a liver donor, according to the standard criteria of Centro Nazionale Trapianti, as previously described [14, 16]. Isolated HLSCs were cultured in the presence of minimal essential medium (α-MEM; Lonza, Basel, Switzerland) supplemented with 10% FCS (Euroclone, MI, Italy), 10 ng/mL human recombinant EGF (Miltenyi, Bergisch Gladbach, Germany), 10 ng/mL human recombinant basic fibroblast growth factor (Miltenyi, Bergisch Gladbach, Germany), 2 nM L-glutamine (Lonza, Basel, Switzerland), and 100 U/mL penicillin/streptomycin (Sigma, St. Louis, MO, USA) and maintained in a humidified 5% CO_2 incubator at 37°C. After 2 weeks, HLSC colonies were expanded and characterized as previously described [16]. Mycoplasma absence was routinely tested using RT-PCR.

2.3 HLSC-EVs isolation and characterization

For EV isolation, sub-confluent HLSCs were cultured overnight in serum-free α-MEM (Lonza, Basel, Switzerland), the supernatant was then recovered and centrifuged for 20 min at 3000 g before

being filtered (0.22 μm filters, Merck-Millipore, Burlington, MA, USA) in order to remove cell debris and apoptotic bodies. Supernatants were then ultracentrifuged (Beckman Coulter Optima L-90 K, Fullerton, CA, USA) at 100000 g for 2 hours at 4 °C. HLSC-EVs were resuspended in RPMI supplemented with 1% dimethyl sulfoxide (DMSO, Sigma-Aldrich, St.Louis, MO, USA) and stored at –80 °C for later use. Nanosight LS300 system (Malvern Panalytical, Malvern, UK) was used to evaluate EVs concentration and size distribution. Briefly, EV preparations were diluted (1:200) in sterile saline solution and analysed by the Nanoparticle Analysis System using the NTA 1.4 Analytical Software, as previously described [12, 14].

2.4 Electroporation protocol.

HLSC-EVs were electroporated using Invitrogen Neon Kit (Invitrogen, Carlsbad, CA, USA), as previously described [10]. Briefly, $6X10^{10}$ EVs were electroporated with a voltage of 750V using a pulse width of 20 ms, for 10 pulses, according to the manufacturer's protocol. EVs were then was incubated for 30 min at 37°C, washed by ultracentrifugation at 100,000g for 2 h at 4°C, resuspended in RPMI (Lonza, Basel, Switzerland) and immediately used for selected experiments. For each experiment, $6X10^{10}$ HLSC-EVs were subjected to 37°C incubation and ultracentrifugation without electroporation to be used as control.

2.5 Coincubation protocol

EVs (10^{10}) were incubated for 1h at 37°C with 100 picomoles of the indicated miRNA, in a final volume of 200 μl RPMI (Lonza, Basel, Switzerland). When indicated, coincubation was followed by RNAse-A (LifeTechnologies, Carlsbad, CA, USA) treatment (0.1 ng/μl) for 3h at 37°C to digest free miRNA. RNAse digestion was stopped by incubation with 4U of RNAse inhibitor (Invitrogen, Carlsbad, CA, USA) for 1h at 37°C. When indicated, RNAse treatment was followed with trypsin digestion (5 ng/ml, 1h at 37°C) (Sigma-Aldrich, St.Louis, MO, USA). Samples were then subjected to centrifugation (4000 RPM, 5 min at 4°C) using 50 kDa filters (Merck-Millipore, Burlington, MA, USA), in order to remove unbound and undigested miRNAs, and immediately used for indicated experiments.

2.6 Cytofluorimetric EV analysis

HLSC-EVs were bound to surfactant-free white aldehyde/sulfate latex beads 4% w/v, 4 μm diameter (Molecular Probes, Thermo Fisher, Waltham, MA, USA) for the cytofluorimetric analysis using Guava instrument (Merck-Millipore, Burlington, MA, USA). Thirty μg of EVs were incubated with five μl of beads for 30 minutes at room temperature and subsequently for 30 minutes at +4°. Adsorbed EVs were then incubated with FITC and PE labelled antibodies against CD63, CD44, integrin alpha 4 and CD29 (all from Beckton Dickinson, Franklin Lakes, NJ, USA) with a final dilution of 1:50, for 15 minutes at +4°C. During the cytofluorimetric acquisition the gating strategy was set on the physical parameters dot plot. Controls corresponded to EVs adsorbed on beads and marked with FITC-, PE- or APC- conjugated mouse IgG1 Isotypes (all purchased by Miltenyi, Bergisch Gladbach, Germany).

2.7 Apoptosis

Cytofluorimetric evaluation of apoptotic cells was performed using the Muse™ Annexin V & Dead Cell Kit (Merck-Millipore, Burlington, MA, USA), according to manufacturer's instructions. Briefly, $10x10^3$ cells were incubated with $50x10^3$ EVs/target cell for 48 hours. Cells were then detached and resuspended in Muse™ Annexin V & Dead Cell Kit (Luminex, Austin, TX, USA), and the percentage of apoptotic cells (Annexin V^+) was detected.

2.8 Invasion

Invasion assay was performed using 24-well cell culture inserts (Beckton Dickinson, Franklin Lakes, NJ, USA) with a porous membrane (8.0 μm pore size) precoated with 100 μg growth factor-reduced Matrigel (Beckton Dickinson, Franklin Lakes, NJ, USA) per well, as previously described [14]. Briefly, $50x10^3$ rCSCs were detached using a non-enzymatic solution (Sigma-Aldrich, St.Louis, MO, USA), and plated in the presence of $50x10^3$ EVs/target cell in the upper side of the pre-coated transwell in DMEM (Euroclone, MI, Italy). As attractive stimulus, complete culture medium was added in the well. Every condition was performed in triplicate. After 48h, cells that moved from the upper side of the transwell to the lower one, were fixed in MetOH and stained with crystal violet (Sigma-Aldrich, St.Louis, MO, USA). Total area of invaded Matrigel (original magnification: 100X) was evaluated by ImageJ on at least five pictures per transwell.

2.9 Super-resolution microscopy

Super-resolution analyses were performed using a Nanoimager S Mark II microscope from ONI (Oxford Nanoimaging) equipped with 405 nm/150mW, 473 nm/1W, 560 nm/1W, 640 nm/1W lasers and dual emission channels split at 640nm. For the preparation of the sample, 10 μl of Poly-L-Lysine (Sigma-Aldrich, St.Louis, MO, USA) was placed on coverslips, in culture wells (Grace Bio-Labs, Sigma-Aldrich, St.Louis, MO, USA), and left for at 37°C in a humidifying chamber for two hours. After removal of the excess, HLSC-EVs previously coincubated with a Scrambled-FITC RNA sequence and digested with RNase, were left to attach overnight at +4°C on the coverslips. Next day, non-attached EVs were removed and 10 μl of blocking buffer (PBS-5% Bovine Serum Albumin) was added into the wells for 30 min. 2.5 μg of purified mouse anti-CD29 antibody (Beckton Dickinson, Franklin Lakes, NJ, USA) were conjugated with Alexa Fluor 647 dye, using the Apex Antibody Labeling Kit (Invitrogen, Carlsbad, CA, USA) according to the manufacturer's protocol. Anti-CD29 Alexa Fluor 647 antibody was added to the blocking buffer containing wells at a final dilution 1:10. The antibody was left for overnight incubation at +4°C. The samples were washed twice with PBS and 10 μl ONI BCubed Imaging Buffer was added for the EV imaging. Two-channel dSTORM data were acquired sequentially at 30 Hz (Hertz) in total reflection fluorescence (TIRF) mode. Single molecule data was filtered using NimOS (Version 1.7.1.10213, ONI) based on point spread function shape, photon count and localization precision to minimize background noise and remove low precision localizations.

2.10 EV incorporation in target cells

To evaluate the internalization of coincubated EVs in rCSCs by fluorescent microscopy, HLSC-EVs were labelled with 1 μM Dil dye (ThermoFisher, Waltham, MA, USA) as described previously [12]. Briefly, HLSC-EVs were resuspended in PBS supplemented with 1 μM Dil dye and ultracentrifuged at 100,000 g for 1 h at 4 °C. EVs were then washed with PBS by ultracentrifugation (100,000 g for 1 h at 4 °C). The EV pellet was resuspended in RPMI and processed for coincubation. Coincubated EVs were immediately used to treat previously plated rCSCs ($50X10^3$ EVs/target cell) for 1h, cells were then fixed in 4% paraformaldehyde (Sigma-Aldrich, St.Louis, MO, USA) and processed for confocal microscopy.

2.11 miRNA isolation and Real time PCR

Total RNA was isolated from different rCSCs or EVs preparations using MirVana kit (Ambion, ThermoFisher, Waltham, MA, USA), according to the manufacturer's protocol, and quantified spectrophotometrically (Nanodrop ND-1000, ThermoFisher, Waltham, MA, USA). First-strand cDNA was produced from 200 ng of total RNA using the miScript Reverse Transcription Kit (Qiagen, Hilden, Germany). Real-time PCR experiments were performed in 20 μl reaction mixture containing 5 ng of cDNA template, the sequence-specific oligonucleotide primers (purchased from MWG-Biotech, Nantes, BRU, Luxembourg) and the miScript SYBR Green PCR Kit (Qiagen, Hilden, Germany). RNU48 was used to normalize miRNA inputs.

2.12 Protein extraction and Western blot

Different preparations of HLSC-EVs were lysed in RIPA buffer supplemented with protease and phosphatase inhibitor cocktail and PMSF (Sigma- Aldrich, St.Louis, MO, USA) immediately after ultrancentrifuge. Aliquots of EV lysates containing 30 μg proteins, as determined by Bradford quantification (Biorad, Hercules, CA, USA), were run on 4-20% SDS-PAGE under reducing conditions and blotted onto PVDF membrane filters using the iBLOT system (LifeTechnologies, Carlsbad, CA, USA). Membranes were blocked in Tris-buffered saline-Tween (TBS-T; 25 mM Tris, pH 8.0, 150 mM NaCl, and 0.05% Tween-20) containing 5% (w/v) non-fat dried milk for 1 h. After blocking, membranes were incubated overnight with anti-ANAXA2 antibody (LS-C150122, LSBio, Seattle, WA, USA). Blots were then incubated with Goat anti-Rabbit IgG HRP conjugated (Thermo Scientific, Waltham, MA, USA) for 1 h at room temperature. Membranes were then probed with ClarityTM Western ECL substrate (Bio-rad, Hercules, CA, USA), and bands were detected by the Chemidoc system (Bio-rad, Hercules, CA, USA).

2.13 Statistical analysis

Statistical analysis was carried out on Graph Pad Prism version 5.04 (Grap Pad Software, Inc, USA) by using the Student t-test or ANOVA with Dunnet's multi-comparison tests, as appropriate. A p value <0.05 was considered significant.

3. Results

3.1 Comparison between electroporation and coincubation to increase the EV antitumor effect

We previously demonstrated the anti-tumor effect of HLSC-EVs on renal cancer stem cells (rCSCs) [12-14]. With the aim of potentiating this effect, we decided to enrich EVs with anti-tumor miRNAs, known to display a strong anti-invasive and pro-apoptotic effect in rCSCs [14]. For this aim, we performed parallel experiments in which we compared EV miRNA loading using electroporation, previously set in our laboratory [10], or coincubation, already reported to be effective [7] on induction of rCSCs apoptosis.

We first assessed the maintenance of functional properties in EVs after coincubation with a scrambled RNA sequence in comparison with electroporation, in the absence of miRNA loading, by testing their biological activity on rCSCs apoptosis induction [12] (Suppl. Fig 1 A). Electroporated EVs showed reduced pro-apoptotic activity, when compared to naïve HLSC-EVs, as already reported [12]. In addition, electroporated EVs were unable to induce the endogenous expression of miR-200a and miR-200b known to be responsible for the anti-tumor effect of naive EVs [14], suggesting loss of active cargo in electroporated EVs (Suppl. Fig. 1 B). At variance, EVs coincubated with a scrambled sequence maintained their pro-apoptotic effect (Suppl. Fig. 1 A), together with the induction of the expression of anti-tumor miRNAs (Suppl. Fig. 1 B).

We therefore decided to set a coincubation protocol for the direct loading of the anti-tumor miRNA miR-145, that is present in low level in naïve HLSC-EVs [14]. In particular, we focused on assessing whether miR-145 loading could potentiate the effect of HLSC-EVs on reduction of the high invasive property of rCSCs [14]. HLSC-EVs incubated with different doses of a scrambled sequence (EV + SCR 100/30/10 picomol, corresponding to 6000/2000/600 miR-molecules/EV) maintained the anti-invasive effect on rCSCs (Fig. 1 A and B), at levels comparable to naïve EVs. Subsequently, generation of miR-145 loaded EVs by coincubation with miR-145 potentiated the anti-tumor effect of naive EVs in terms of invasion (Fig. 1 A and B). In particular, different doses of miR-145 tested (EV-145 100/30/10 pmol/1010 EVs, corresponding to 6000/2000/600 miR-molecules/EV, red bars), increased the anti-invasive effect of naïve EVs, being the higher dose (100 picomol/1010 EVs) the most efficient. This dose was selected for the following experiments. MiR-145 alone, used as control, at the highest dose (100 picomol/1010 EVs, corresponding to 6000 miR-145 molecules/EV), also exerted an anti-invasive effect (Fig. 1 A and B), since miRNA molecules could aggregate during EV engineering, as previously shown [17].

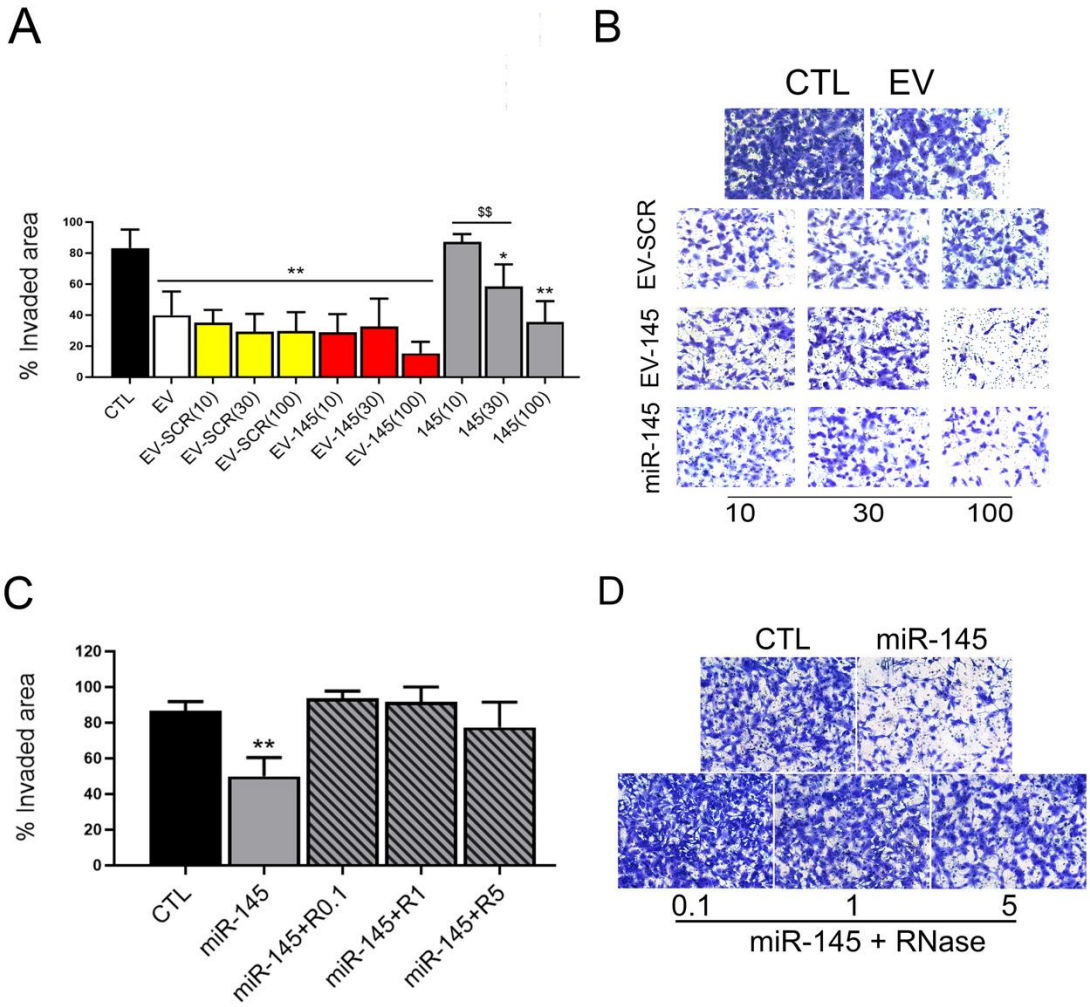

Fig. 1. **Effect of miR145 coincubated HLSC-EVs on rCSC invasion**. A and B: Quantification (A) and representative micrographs (original magnification: X100) (B) of rCSCs invasion after treatment for 48h with HLSC-EVs (EV) loaded with different doses (100/30/10 pmol/10^{10} EVs, corresponding to 6000/2000/600 molecules/EV) of a scrambled sequence (EV-SCR) or with miR-145 (EV-145), or with miR-145 alone (145); all at the dose of 10, 30 or 100 pmol/10^{10} EVs. Data are represented as mean ± SD of the percentage of invaded area of three experiments. C and D: Invasion assay quantification (D) and representative micrographs (original magnification: X100) (E) of rCSCs treated for 48h with miR-145 untreated (miR-145) or digested with 0.1, 1 or 5 ng/µl of RNase-A (miR-145+R0.1, 1 or 5 respectively). Data are represented as mean ± SD of the percentage of invaded area of three experiments.

3.2. RNAse treatment of coincubated EVs

In order to obtain miR-145 coincubated EVs in the absence of unbound miR-145, we took advantage of RNAse treatment. Indeed, incubation of miR-145 alone with 0.1, 1 or 5 µg/ml RNAse abolished the observed anti-invasive effect, indicating its susceptibility to RNAse treatment at all doses (Fig. 1 C and D). We therefore chose the lowest RNAse concentration (0.1 µg/ml) to digest the unbound fraction of miR-loaded EVs.

We first assessed EV integrity after RNAse treatment by NTA (Fig. 2 A) and super resolution microscopy (Fig. 2 B). As shown in Fig. 2 A, the size distribution of coincubated EVs treated with RNAse did not vary in respect to naive EVs. In addition, super resolution microscopy images of HLSC-EVs coincubated with a FITC-scrambled sequence, confirmed the effective RNA loading and maintenance after RNAse treatment (Fig. 2 B). Moreover, EV uptake by rCSCs was not affected (Fig.

2 C). In order to assess whether EV coincubation and/or RNAse treatment could affect EV protein content, we performed flow cytometry analysis on HLSC-EVs, evaluating the percentage of EVs positive for different EV markers (CD44, CD29, integrin alpha4 (A4), CD81, CD63), known to be present on HLSC-EVs. As shown in Fig. 2 D, we did not detect any change in marker expression, suggesting that EV integrity was maintained.

3.3 Anti-tumor effect and miR145 transfer of RNase treated coincubated EVs

We therefore applied the above described protocol of coincubation and digestion of unbound miRNA with RNAse to enrich HLSC-EVs with the anti-tumor miR-145. In order to assess whether engineered HLSC-EVs could transfer miR-145 to target cells, we treated rCSCs with miR-145-loaded EVs ($50x10^3$/cell) and we analysed miR-145 levels in rCSCs after 24 and 48h of EV treatment. As shown in Fig. 2 E, naïve HLSC-EVs (EV) did not induce in rCSCs any detectable change of miR-145 expression respect to untreated cells (CTL), while we observed a 100-fold increase in miR-145 levels when rCSCs were incubated with HLSC-EVs loaded with miR-145 (EV-miR145). RNAse treatment did not interfere with miR-145 transfer, since the same increase was observed when coincubated EVs were treated with RNAse (EV-miR145+RNAse). In order to evaluate if the observed increase of miR-145 in target cells was due to a miR-145 transfer and not to its induction, we analysed the levels of pre-miR-145 in rCSCs treated with HLSC-EVs coincubated with miR-145 (EV-miR145). As shown in Fig. 2 F, no detectable change in pre-miR145 was observed, further suggesting miR-145 transfer in rCSCs by HLSC-EVs coincubated with miR-145. At variance, transfer of free unbound miR-145 levels (miR-145, yellow bar) was reduced after RNAse treatment (miR-145+RNAse), indicating the degradation of free miR-145 by RNAse.

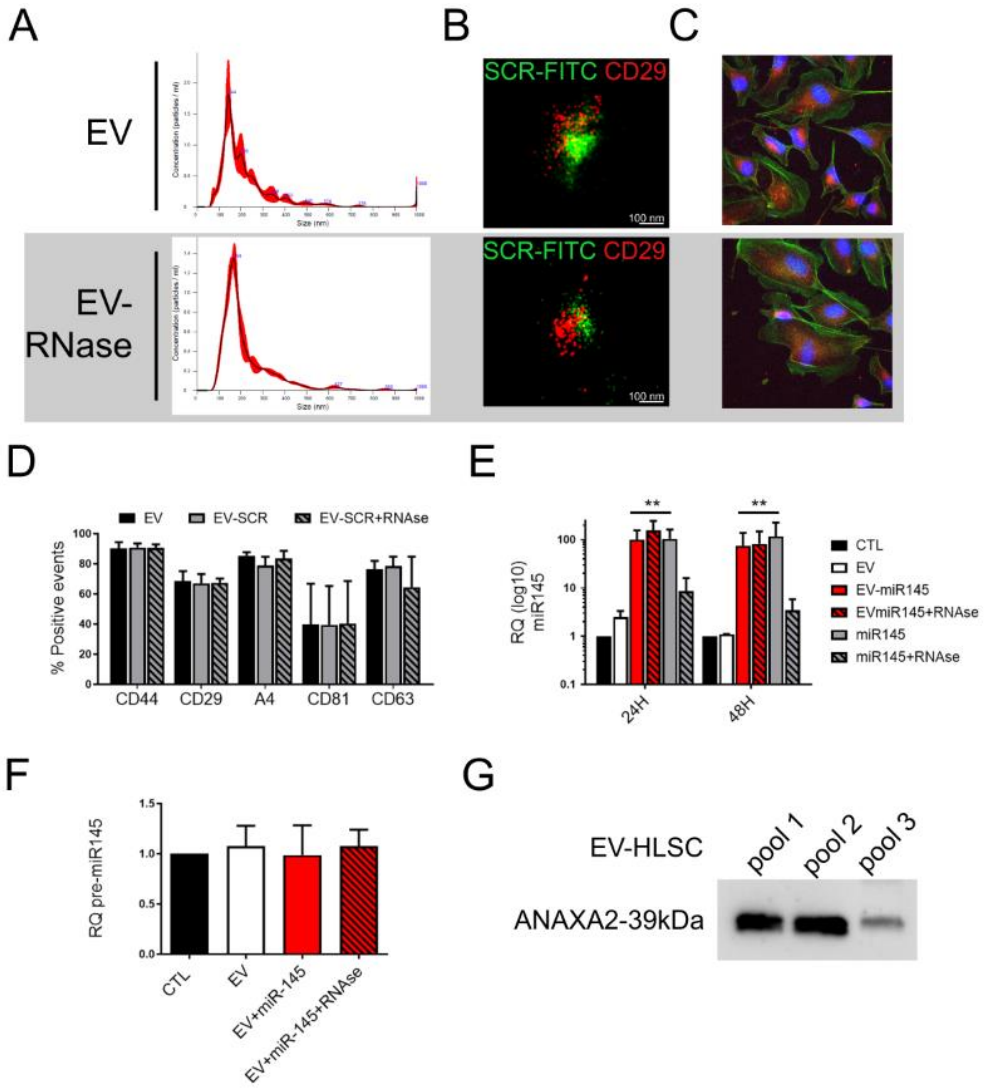

Figure 2. Integrity of miR145 coincubated HLSC-EVs after RNase treatment. A: NanoSight distribution graph showing the quantity and size of HLSC-EVs untreated (Pre-RNase) or digested with 0.1 ng/µl RNase-A (RNase 0.1 ng/µl). B: Super resolution microscopy micrographs showing the effective loading of a scrambled FITC sequence (green). HLSC-EVs are labelled with anti-CD29 Ab (red). Scale bar: 100 nm. C: Representative micrographs of incorporation of DIL-labelled HLSC-EVs (EV) and DIL-labelled HLSC-EVs treated with 0.1 ng/µl RNase-A (EV-RNase) in rCSCs after 1 hour of incubation detected by confocal microscopy (Original magnification x400). D: Immunophenotypic characterization of HLSC-EVs (EV) loaded with a scrambled sequence (EV-SCR) and treated with 0.1 ng/µl RNase-A (EV-SCR+RNase), expressing the markers of cells of origin (CD44, CD29 and integrin alpha4 (A4)), together with the exosomal markers CD63 and CD81. Results are mean ± SD of the percentage of positive events of four different independent EV preparations. E: Real Time analysis showing miR-145 levels in rCSCs treated for 24h or 48h with naïve HLSC-EVs (EV), HLSC-EVs coincubated with miR-145 untreated (EV-miR145) or digested with 0.1 ng/µl RNase-A (EV-miR145+RNAse), or with free miR-145 untreated (miR145) or digested with 0.1 ng/µl RNase-A (miR145+RNAse). Data are represented as mean ± SD of four independent experiments of the Relative Quantification (RQ) normalized to untreated cells (CTL) and to RNU6B. One-way ANOVA was performed: **=p<0.001 vs CTL. F: Real Time analysis showing pre-miR-145 levels in rCSCs treated for 24h with naïve HLSC-EVs (EV), HLSC-EVs coincubated with miR-145 untreated (EV-145) or digested with 0.1 ng/µl RNase-A (EV-145+RNAse). Data are represented as mean ± SD of three independent experiments of the Relative Quantification (RQ) normalized to untreated cells (CTL) and to RNU6B. G: Western blot analysis of three different HLSC-EVs preparations (pool1, pool2, pool3) showing the presence of Annexin A2 (ANAXA2).

3.4 Protection of surface loaded miRNAs by RNA binding proteins

To understand the mechanism of RNAse protection of miR-145 on HLSC-EV surface, we hypothesized the presence of surface RNA-binding proteins that could act to protect bound miRNAs. As shown in Fig. 2 G, HLSC-EVs expressed Annexin A2 (ANXA2), known to play an active role in miRNA-loading in EVs [18], and to be present on EV surface [19].

To further confirm the possible involvement of surface RNA-binding proteins in miRNA loading and protection, we treated EVs with trypsin. As shown in Fig. 3 A, trypsin treatment did not interfere with EV anti-invasive activity. We therefore evaluated miR-145 levels in HLSC-EVs (EV), EV coincubated with miR-145 (EV-miR145) and treated for 3h with RNAse (EV-145+RNAse) and for an additional 1h with trypsin (EV-145+RNase+TR). As shown in Figure 3 B, the enrichment of miR-145 within EVs was high after co-incubation and resistant to RNAse treatment but it was significantly abolished after trypsin treatment, further suggesting that miR-145 is bound to RNA-binding proteins present in EV surface.

In addition, we tested the effect of EVs coincubated with miR-145 on the invasion ability of rCSCs, (Fig. 3 C and D). The effect of naïve EV was increased when EVs were coincubated with miR-145 as expected (EV-miR145). EV treatment with RNAse did not reduce the effect of miR-145 coincubated EVs (EV-miR145+RNAse), while it reduced that of free miR-145 (miR-145+RNAse). Trypsin treatment of coincubated EVs (EV-miR145+TR) reverted the effect of EV-miR145, confirming at a functional level the role of membrane RNA-binding proteins on EV loading with anti-tumor miRNAs by coincubation.

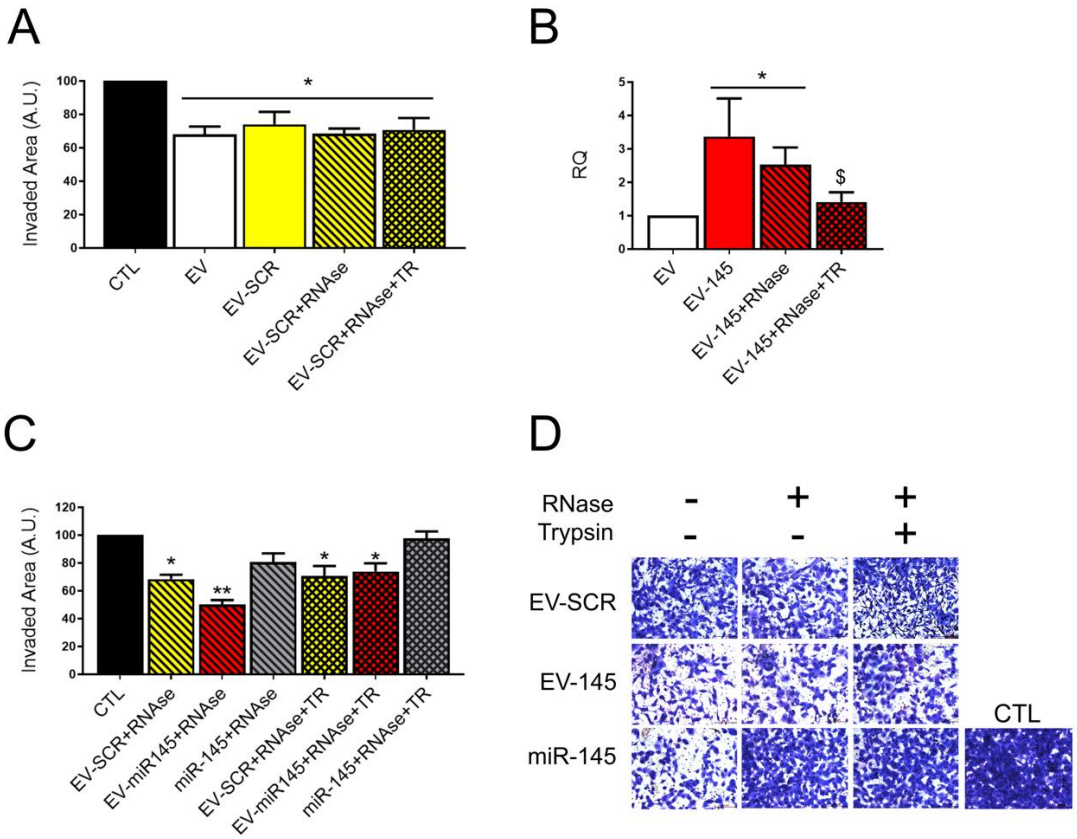

Figure 3. **Anti-tumor effect of miR145 coincubated HLSC-EVs after RNase but not trypsin treatment**. A: Invasion assay quantification of rCSCs treated for 48h with naïve HLSC-EVs (EV), or with HLSC-EVs coincubated with a scrambled sequence (EV-SCR), EV-SCR digested with RNase-A (EV-SCR+RNase) and EV-SCR treated with RNase. Data are represented as mean of the percentage of invaded area of one

experiment performed in triplicate. B: Real Time analysis showing miR-145 levels in naïve HLSC-EVs (EV), HLSC-EVs coincubated with miR-145 untreated (EV-145) or digested with 0.1 ng/µl RNase-A (EV-145+RNAse), or digested with RNase and treated with trypsin (EV-145+RNase+TR). Data are represented as mean ± SD of three independent experiments of the Relative Quantification (RQ) normalized to naïve EVs (EV) and to RNU6B. *=p<0.05 vs EV and $=p<0.05 vs EV-145. C and D: Invasion assay quantification (D) and representative micrographs (E) of rCSCs treated for 48h with naïve HLSC-EVs (EV), or with HLSC-EVs coincubated with a scrambled sequence or with miR-145 and digested with RNase-A (EV-SCR+RNase and EV-miR145+RNase respectively), or with EV-SCR+RNase and EV-miR145+RNase treated with trypsin (EV-SCR+RNase+TR and EV-miR145+RNase+TR respectively). Free miR-145, treated with RNase (miR145+RNase) or with RNase and trypsin (miR145+RNase+TR) was used as control. Data are represented as mean of the percentage of invaded area of two experiments performed in triplicate. A-Nova was performed: *=p<0.05 and **=p<0.001 vs untreated rCSCs (CTL).

3.5 Coincubation protocol using antitumor miRNAs

Finally, we tested the *in vitro* effect of HLSC-EVs coincubated with all the anti-tumor miRNAs previously identified as mediators of the anti-tumor effect of HLSC-EVs [14] (miR-145, miR-200b, miR-200c, miR-223 and miR-429). Coincubated EVs were subsequently treated with RNAse in order to exclude any affect due to unbound miRNA. As shown in Fig. 4, we observed an additive anti-invasive effect, respect to naïve EVs, when EVs were coincubated with miR-145 or miR-429.

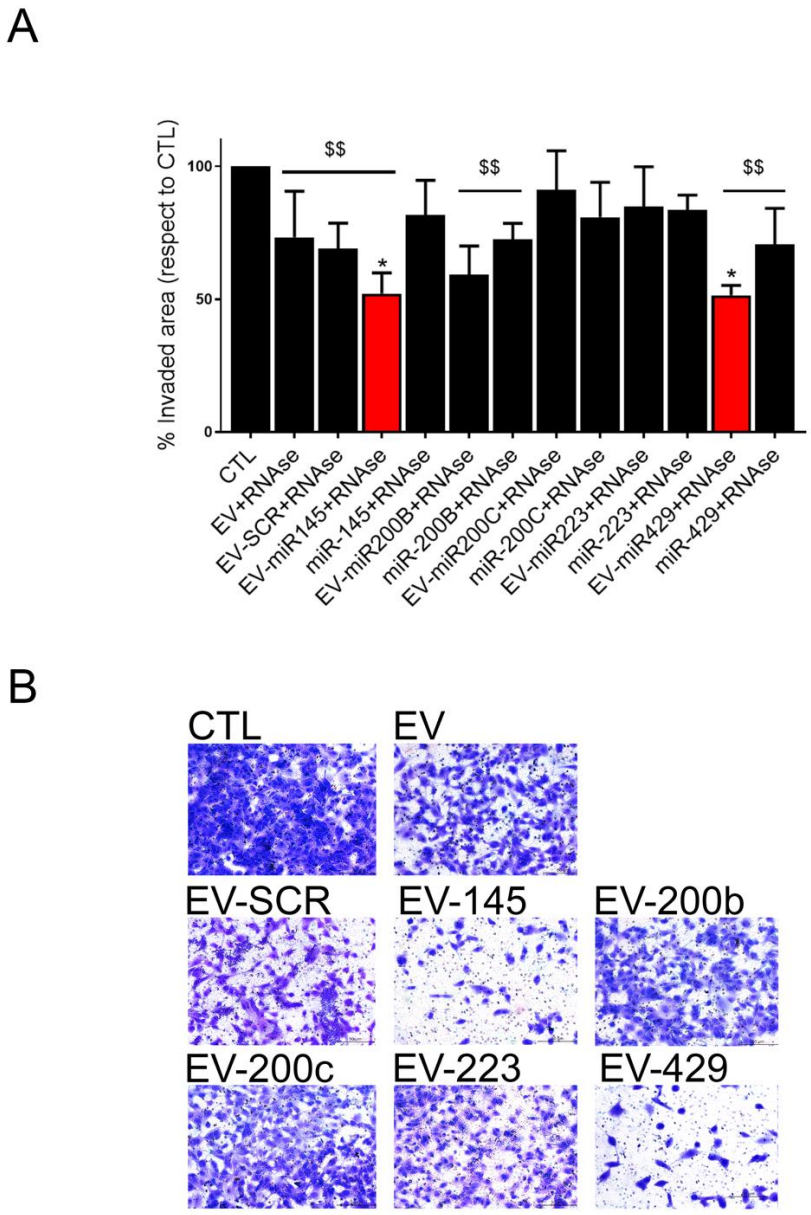

Figure 4.: Anti-invasive effects of Coincubation Invasion assay quantification (A) and representative micrographs (B) of rCSCs treated for 48h with naïve HLSC-EVs (EV), or with HLSC-EVs coincubated with a scrambled sequence or with anti-tumor miRNAs (miR-145, miR200b, miR200c, miR223 and miR429) and digested with RNase-A (EV-miR+RNase). miRNAs alone digested with RNase were used as controls (miR+RNase). Data are represented as mean of the percentage of invaded area of at least two experiments performed in triplicate. A-Nova was performed: *=$p<0.05$ vs EV; $$=$p<0.001$ vs untreated rCSCs (CTL).

4. Discussion

In the present study, we successfully set up a co-incubation protocol able to load microRNAs on HLSC-EVs surface. Engineered co-incubated HLSC-EVs efficiently delivered microRNAs, that were indeed protected by RNase, promoting microRNA specific functions while maintaining the desired effect of naïve EVs on rCSC. The ability of EV to bind and transport active RNA and DNA species on their surface is a well-known phenomenon [1, 4]. In particular, EVs circulating in serum and present in other biological fluids contain surface-bound nucleic acids within their corona that are considered contaminants. In some cases, additional treatment may be required to remove them from the outside surface of EVs using RNase or DNase [20]. However, membrane bound RNA species are likely to be protected from RNase degradation, considering the high levels of RNase in biological media such as blood plasma. Indeed, recent reports suggest an active effect of EV surface-associated DNA in horizontal gene transfer of EVs released by mesenchymal stem cells [21, 22].

In the present study, we reasoned to exploit the EV ability of binding, protecting and delivering nucleic acids to set up a method for EV engineering. The in vitro assessment of rCSCs invasion was chosen as readout to compare the effect described for naïve HLSC-EVs [14] with that of engineered HLSC-EVs, in virtue of the simplicity and effectiveness of this test. Considering preliminary experiments showing the loss of biological effect of naïve HLSC-EVs using electroporation, we decided to set up a different protocol able to maintain EV integrity. Indeed, it is conceivable that the electroporation process itself might generate loss of EV membrane integrity with exit of active components, such as RNA species, simultaneously to the entrance of the desired miRNAs. Moreover, several publications have described difficulty in the application of the engineering approach with electroporation because of a high degree of variability [23], though an effective *in vivo* silencing of the target gene.

To increase the therapeutic effect of HLSC-EVs, we here chose miR-145. In fact, miR-145 is an antitumor miRNA, known to be downregulated in renal cancer [24]. We recently shown that transfection of rCSCs with miR-145 results in apoptosis induction and tumor cell invasion reduction [14]. Moreover, the transfer of anti-tumor miRNAs to rCSCs, mediated by HLSC-EVs, was able to induce in cancer cells the expression of miR-200 family members, involved in metastasis formation, both *in vitro* and *in vivo* [14]. The loading of another anti-tumor microRNA, such as miR-145, in HLSC-EVs, resulting in the increase of miR-145 levels in HLSC-EVs, could therefore potentiate the observed anti-tumor effect on rCSCs.

The effective loading of miR-145 and its maintenance after RNase treatment was demonstrated trough microRNA expression in HLSC-EVs, transfer with increase of its level in target cells, and with super resolution microscopy. Using the coincubation protocol, we successfully generated HLSC-EVs with an enhanced effect on the reduction of rCSC invasion. Interestingly, miR-145 alone, that was effective *per se* possibly due to its persistence as miRNA aggregates [17], was inactive after RNase treatment. The observed protection of surface-bound microRNA was likely due to the presence of RNA-binding proteins able to protect bound miRNAs. In particular, we identified the expression on HLSC-EV surface of ANXA2, known to play an active role in miRNA-loading in EVs [18]. This RNA binding protein was previously described on human pancreatic cancer EV surface [19]. The possible involvement of surface RNA-binding proteins in miRNA loading and protection was confirmed by the loss of their activity after trypsin treatment. In conclusion, we consider that active naïve EVs, such as those of MSCs and other stem cell types, could be an interesting therapeutic EV source for additional engineering. The protocol reported here might therefore be of interest in these situations, exploiting a well described property of EVs to bind nucleic acids on their surface and protect them from degradation. Further studies will be required to assess the effective microRNA delivery of engineered EVs in *in vivo* settings.

Supplementary Materials: The following are available online at www.mdpi.com/xxx/s1, Figure S1: Comparison of electroporation and coincubation EV protocol on rCSC apoptosis and miR transfer.

Author Contributions: Conceptualization, AB, GC and BB.; experimental procedures AB, MT, VF, EP, MD; data analysis AB; writing—original draft preparation, AB and BB.; writing—review and editing, AB, GC and BB. All authors have read and agreed to the published version of the manuscript.

Funding: This study was supported by Associazione Italiana per la Ricerca sul Cancro (A.I.R.C.), project IG2015 16973 and by grant no. 071215 from Unicyte to GC and BB.

Acknowledgments: The authors thank Unicyte AG for providing HLSC.

Conflicts of Interest: The authors declare no conflict of interest.

References

[1] Camussi, G.; Deregibus, MC.; Bruno, S.; Grange, C.; Fonsato, V.; Tetta, C. Exosome/microvesicle-mediated epigenetic reprogramming of cells. *Am J Cancer Res.* 2011, *1(1)*, 98-110.
[2] Raposo, G.; Stoorvogel, W. Extracellular vesicles: exosomes, microvesicles, and friends. *J Cell Biol.* 2013, *200(4)*, 373-83.
[3] Turturici, G.; Tinnirello, R.; Sconzo, G.; Geraci, F. Extracellular membrane vesicles as a mechanism of cell-to-cell communication: advantages and disadvantages. *Am J Physiol Cell Physiol.* 2014, *306(7)*, C621-33.
[4] Massaro, C.; Sgueglia, G.; Frattolillo, V.; Baglio, SR.; Altucci ,L.; Dell'Aversana, C. Extracellular Vesicle-Based Nucleic Acid Delivery: Current Advances and Future Perspectives in Cancer Therapeutic Strategies. *Pharmaceutics*. 2020, *12(10)*, 980.
[5] Stremersch, S.; Vandenbroucke, RE.; Van Wonterghem, E.; Hendrix, A.; De Smedt, SC.; Raemdonck, K. Comparing exosome-like vesicles with liposomes for the functional cellular delivery of small RNAs. *J Control Release.* 2016, *232*, 51-61.
[6] Johnsen, KB.; Gudbergsson, JM.; Duroux, M.; Moos, T.; Andresen, TL.; Simonsen, JB. On the use of liposome controls in studies investigating the clinical potential of extracellular vesicle-based drug delivery systems - A commentary. *J Control Release*. 2018, *269*, 10-14.
[7] O'Loughlin AJ.; Mäger, I.; de Jong, OG.; Varela, MA.; Schiffelers, RM.; El Andaloussi, S.; Wood, MJA.; Vader, P. Functional Delivery of Lipid-Conjugated siRNA by Extracellular Vesicles. *Mol Ther.* 2017, *25(7)*,1580-1587.
[8] Devhare ,PB.; Ray, RB. A novel role of exosomes in the vaccination approach. *Ann Transl Med*. 2017, *5(1)*, 23.
[9] Sutaria, DS.; Badawi, M.; Phelps, MA.; Schmittgen, TD. Achieving the Promise of Therapeutic Extracellular Vesicles: The Devil is in Details of Therapeutic Loading. *Pharm Res.* 2017, *34(5)*, 1053-1066.
[10] Pomatto, MAC.; Bussolati, B.; D'Antico, S.; Ghiotto, S.; Tetta, C.; Brizzi, MF.; Camussi, G. Improved Loading of Plasma-Derived Extracellular Vesicles to Encapsulate Antitumor miRNAs. *Mol Ther Methods Clin Dev*. 2019, *13*, 133-144.
[11] Fonsato, V.; Collino, F.; Herrera, MB.; Cavallari, C.; Deregibus, MC.; Cisterna, B.; Bruno, S.; Romagnoli, R.; Salizzoni, M.; Tetta, C.; Camussi, G. Human liver stem cell-derived microvesicles inhibit hepatoma growth in SCID mice by delivering antitumor microRNAs. *Stem Cells*. 2012, *30(9)*,1985-1998.
[12] Fonsato, V.; De Lena, M.; Tritta, S.; Brossa, A.; Calvetti, R.; Tetta, C.; Camussi, G.; Bussolati, B. Human liver stem cell-derived extracellular vesicles enhance cancer stem cell sensitivity to tyrosine kinase inhibitors through Akt/mTOR/PTEN combined modulation. *Oncotarget*. 2018, *9(90)*, 36151-36165.
[13] Lopatina, T.; Grange, C.; Fonsato, V.; Tapparo, M.; Brossa, A.; Fallo, S.; Pitino, A.; Herrera-Sanchez, MB.; Kholia, S.; Camussi, G.; Bussolati, B. Extracellular vesicles from human liver stem cells inhibit tumor angiogenesis. *Int J Cancer.* 2019, *144(2)*, 322-333.
[14] Brossa, A.; Fonsato, V.; Grange, C.; Tritta, S.; Tapparo, M.; Calvetti, R.; Cedrino, M.; Fallo, S.; Gontero, P.; Camussi, G.; Bussolati B. Extracellular vesicles from human liver stem cells inhibit renal cancer stem cell-derived tumor growth in vitro and in vivo. *Int J Cancer*. 2020, *147(6)*, 1694-1706.
[15] Bussolati, B.; Bruno, S.; Grange, C.; Ferrando, U.; Camussi, G. Identification of a tumor-initiating stem cell population in human renal carcinomas. *FASEB J.* 2008, *22(10)*, 3696-705.
[16] Herrera, MB.; Bruno, S.; Buttiglieri, S.; Tetta, C.; Gatti, S.; Deregibus, MC.; Bussolati, B.; Camussi, G. Isolation and characterization of a stem cell population from adult human liver. *Stem Cells.* 2006, *24(12)*, 2840-50.
[17] Kooijmans, SAA.; Stremersch, S.; Braeckmans, K.; de Smedt, SC.; Hendrix, A.; Wood, MJA.; Schiffelers, RM.; Raemdonck, K.; Vader, P. Electroporation-induced siRNA precipitation obscures the efficiency of siRNA loading into extracellular vesicles. *J Control Release*. 2013, *172(1)*, 229-238.
[18] Hagiwara, K.; Katsuda, T.; Gailhouste, L.; Kosaka, N.; Ochiya, T. Commitment of Annexin A2 in recruitment of microRNAs into extracellular vesicles. *FEBS Lett*. 2015, *589(24 Pt B)*, 4071-8.

[19] Stewart, S.; Gessler, F.; Pluchino, S.; Moreau, K. Inside-out: Unpredicted Annexin A2 localisation on the surface of extracellular vesicles. *Matters*. 2016, *10*, 19185.
[20] Mateescu, B.; Kowal, EJ.; van Balkom, BW.; Bartel, S.; Bhattacharyya, SN.; Buzás, EI.; Buck, AH.; de Candia, P.; Chow, FW.; Das, S.; Driedonks, TA.; Fernández-Messina, L.; Haderk, F.; Hill, AF.; Jones JC.; Van Keuren-Jensen KR.; Lai CP.; Lässer C.; Liegro ID.; Lunavat TR.; Lorenowicz MJ.; Maas, SL.; Mäger, I.; Mittelbrunn, M.; Momma, S.; Mukherjee, K.; Nawaz, M.; Pegtel, DM.; Pfaffl, MW.; Schiffelers, RM.; Tahara, H.; Théry, C.; Tosar, JP.; Wauben, MH.; Witwer, KW.; Nolte-'t Hoen, EN. Obstacles and opportunities in the functional analysis of extracellular vesicle RNA - an ISEV position paper. *J Extracell Vesicles*. 2017, *6(1)*, 1286095.
[21] Fischer, S.; Cornils, K.; Speiseder, T.; Badbaran, A.; Reimer, R.; Indenbirken, D.; Grundhoff, A.; Brunswig-Spickenheier, B.; Alawi, M.; Lange, C. Indication of horizontal DNA gene transfer by extracellular vesicles. *PLoS One*. 2016, *29*, 11(9):e0163665.
[22] Shelke, GV.; Jang, SC.; Yin, Y.; Lässer, C.; Lötvall, J. Human mast cells release extracellular vesicle-associated DNA. *Matters*. 2016, *2*, e201602000034.
[23] Wahlgren, J.; De L Karlson, T.; Brisslert, M.; Vaziri Sani, F.; Telemo, E.; Sunnerhagen, P.; Valadi, H. Plasma exosomes can deliver exogenous short interfering RNA to monocytes and lymphocytes. *Nucleic Acids Res.* 2012, *40*, e130
[24] Slaby, O.; Redova, M.; Poprach, A.; Nekvindova, J.; Iliev, R.; Radova, L.; Lakomy, R.; Svoboda, M.; Vyzula, R. Identification of MicroRNAs associated with early relapse after nephrectomy in renal cell carcinoma patients. *Genes Chromosomes Cancer*. 2012, *51(7)*, 707-16